The role of convectively coupled atmospheric Kelvin waves on African easterly wave activity

Michael J. Ventrice[1]
Department of Atmospheric and Environmental Science, University at Albany, Albany, NY

Chris D. Thorncroft
Department of Atmospheric and Environmental Science, University at Albany, Albany, NY

[1] *Corresponding Author Address:* Michael Ventrice, University at Albany, 1400 Washington Avenue, Albany, NY 12222.
E-mail: MVentrice@albany.edu

Abstract:

The role of convectively coupled atmospheric Kelvin waves (CCKWs) on African easterly wave (AEW) activity is explored over tropical Africa during boreal summer. A modulation of the African synoptic environment by the CCKWs is shown to favor the formation and intensification of mesoscale convective systems and AEWs during and after its passage. The pre-Alberto AEW (2000) is investigated as a case study to show that its initiation occurred during the passage of the convectively active phase of an eastward propagating CCKW.

CCKWs modulate the horizontal structure of the African easterly jet (AEJ). The dynamical structure associated with the CCKW has wind anomalies peaked equatorward of the AEJ. Therefore, the CCKW imposes horizontal shear on the AEJ, which modulates the relative vorticity sign-reversal in the jet core. Further, the convectively active phase of the CCKW is shown to increase the climatological background low-level (925-700 hPa) easterly vertical wind shear over Africa, which favors the initiation and growth of organized convection. Due to the modulation of the AEJ by the CCKW and its influence on convective triggers over Africa, AEW activity is assumed to be also modulated by the CCKW.

AEW activity increases after the passage of the convectively active phase of the CCKW over western Africa and during its passage over central-eastern Africa. It is suggested that African topography is important for the localized enhanced AEW activity. These two areas of anomalous AEW activity later move back towards the west over the Atlantic and represent a train of AEWs.

1. Introduction

The impact of African easterly waves (AEWs) on West African rainfall during boreal summer is a well known and heavily studied topic (e.g., Kiladis et al. 2006 and references therein). In addition to having a strong impact on West African rainfall, AEWs are also associated with acting as initial precursors for tropical cyclones over the tropical Atlantic (e.g., Avila and Pasch 1992) and over the Pacific (Frank 1970). Given the large body of work on these waves, it is perhaps surprising that there is still a lack of understanding of when and how these waves originate. During the 1970s, most believed that AEWs formed from a mixed barotropic and baroclinic instability mechanism, which was backed by several idealized modeling studies showing that AEWs could grow from small amplitudes on an unstable African easterly jet (AEJ; e.g., Rennick 1976; Simmons 1977; Thorncroft and Hoskins 1994a,b). But recent work has challenged this hypothesis (e.g., Mekonnen et al. 2006; Kiladis et al. 2006; Hall et al. 2006; Thorncroft et al. 2008). These studies have proposed that AEWs are triggered by some localized forcing that is in the form of latent heating in the entrance region of the AEJ. Thorncroft et al. (2008) suggest that AEWs rely on the presence of significant upstream convective triggers linked to African topography. It is argued here that convectively-coupled equatorial atmospheric Kelvin waves (CCKWs) can provide such triggers over African topographic features by providing a favorable environment for convection and wave growth. This concept provides new insight on a concept that is not yet fully understood and could be used to support the long range prediction of AEW activity.

Mekonnen et al. (2006) and Kiladis et al. (2006) note the importance of the eastern African highlands on AEW genesis. They find that the Darfur Mountains and the Ethiopian Highlands (~35˚E) are preferable regions for AEW genesis. In an idealized modeling study,

Thorncroft et al. (2008) imposed latent heating over an area near the longitude of the Darfur Mountains. While no topographic information was given to the model, the result was a developing train of AEWs that propagated westward with time, providing strong evidence to support that AEWs can be formed by an upstream convective heating in the vicinity of the AEJ entrance.

The modeling studies of Hsieh and Cook (2005) provide an alternative hypothesis regarding the role of convection for the genesis of AEWs. They suggest that latent heating is important for strengthening the potential vorticity (PV) strip on the cyclonic side of the AEJ. This enhanced PV sign reversal provides a more favorable environment for AEW genesis via a linear instability mechanism. By removing latent heating in their model, the associated PV strip did not form and, as a result, AEWs failed to form.

More recently, there has been a general ambition towards understanding the interactions of convection over the elevated terrain of eastern Africa (e.g., Carlson 1969a; Berry and Thorncroft 2005; Mekonnen et al. 2006; Thorncroft et al. 2008). Berry and Thorncroft (2005) suggest that the strong AEW that developed into Hurricane Alberto (2000) was triggered by strong convection over the Darfur Mountains (~25ºE) on July 30-31, 2000. In contrast to this, Hill and Lin (2003) suggest that the pre-Alberto AEW originated from a small-scale (order of 200 km) MCS over the Ethiopian Highlands on July 28th. This MCS was observed to decay prior to the initial convective burst over the Darfur Highlands (Berry and Thorncroft 2005). It will be shown that the increased convection linked to the genesis of the pre-Alberto AEW over the Darfur Mountains occurred during the passage of the convectively active phase of an eastward propagating CCKW.

CCKWs substantially modulate tropical rainfall in the region of the intertropical convergence zone (ITCZ) on synoptic spatial and temporal scales (Gruber 1974; Zangvil 1975; Takayabu 1991; Pires et al. 1997; Wheeler and Kiladis 1999; Wheeler et al. 2000; Mekonnen et al. 2008). Observational studies using high resolution rainfall and brightness temperature datasets (e.g., GOES-9, CLAUS, TRMM 3B42, etc.) reveal that most of the organized rainfall within the convective envelope of the CCKW is composed of smaller scale cloud clusters that move westward (e.g., Straub and Kiladis 2002; Mounier et al. 2007; Mekonnen et al. 2008; Kiladis et al. 2009; Schreck and Molinari 2011; Laing et al. 2011; Tulich and Kiladis 2012). Mounier et al. (2007) observed an increase of MCS activity within the convective envelope of a CCKW over Africa during early July 1984. Their results show that CCKWs are able to modulate convective activity over the whole ITCZ domain by impacting the frequency and intensity of MCSs, with an emphasis over the Cameroon Highlands and central Africa. Laing et al. (2011) also find that MCSs are larger and more intense within the convective envelope of a CCKW.

Mekonnen et al. (2008) observed a strong CCKW passage over Africa during the boreal summer of 1987. Prior to the passage of this strong CCKW, AEW activity was very weak. It wasn't until directly after the passage of the CCKW that AEW activity became significant. However, Mekonnen et al. (2008) suggests that this case was a rare event, such that on average three AEWs initiate per year over Africa during the passage a CCKW. In support of CCKWs modulating AEW activity, Leroux et al. (2010) suggest that intraseasonal variability of AEW activity can vary with eastward propagating modes such as CCKWs and or the MJO. These eastward propagating disturbances are suggested to impact the characteristics of the AEJ, which thereafter would impact AEW activity.

This paper is motivated by the hypothesis of Mekonnen et al. (2008) that CCKWs could occasionally act as convective triggers for initiating AEWs. This work will extend upon Mekonnen et al. (2008) and provide further detail on how CCKWs affect AEW genesis and growth. In the case of a pre-existing AEW, the superposition with the convectively active phase of the CCKW is assumed to amplify the AEW by increasing latent heating within the wave. This paper is constructed as follows. Section 2 discusses the datasets and methodology used. Section 3 considers the role of a CCKW on the initiation of the AEW that later formed into Hurricane Alberto (2000). A composite analysis that investigates the role of CCKWs on atmospheric parameters associated with AEW genesis is in section 4. Discussion and conclusions are included in section 5.

2. Data and Methodology

The European Centre for Medium-Range Weather Forecasts (ECMWF) Re-Analysis (ERA-Interim) dataset (Simmons et al. 2007) was used to investigate the impact of a CCKW passage on the synoptic environment over tropical Africa. This dataset has a horizontal resolution of 1.5° and covers the period 1989 to the present.

Tropical rainfall information associated with the pre-Alberto AEW case study is provided by the TRMM multi-satellite precipitation analysis (TMPA; TRMM product 3B42; Huffman et al. 2007). This dataset merges precipitation estimates from passive microwave sensors on a set of low earth orbiting satellites that are calibrated using global analyses of monthly rain gauge data. This dataset is made available from 1998-present on 3-hourly 0.25˚ latitude-longitude grids, but has been averaged to 6-hourly 1˚ latitude-longitude grids to improve computational efficiency. By averaging the data onto a coarser grid, the missing data was interpolated bilinearly in space and linearly in time from the surrounding values.

Geostationary Earth Orbit infrared (IR) data from the Climate Prediction Center (CPC) merged IR dataset was used to investigate the convective burst over Darfur that has been attributed to as the initiation of the pre-Alberto AEW (Berry and Thorncroft 2005). The CPC-merged IR dataset is a composite of all geostationary earth orbiting IR (~11 μm) images from the multifunctional transport satellite [MTSAT; formerly the geostationary meteorological satellite], Geostationary Operational Environmental Satellite (GOES), and Meteosat satellites (Janowiak et al. 2001). Zenith angle corrections are used to match brightness temperatures away from the respective sub-satellite points. This data is made available at 4 km spatial resolution every 30 minutes.

Following Leroux et al. (2010), AEW activity was diagnosed by calculating the eddy kinetic energy (EKE) based on ECMWF-Interim wind data that were filtered in a 2-10 day band (u' and v'). The EKE, defined as:

$$EKE = \tfrac{1}{2}(u'^2 + v'^2) \quad (1)$$

and was calculated at the level of the AEJ (700 hPa).

The CCKWs used in the composite analysis were identified by filtering National Oceanic and Atmospheric Administration's (NOAA's) daily averaged interpolated outgoing long-wave radiation (OLR) dataset (e.g., Liebmann and Smith 1996) in wavenumber and frequency within the Kelvin band (a period of 2.5-20 days, with eastward wave numbers 1-14, constrained by the Kelvin wave dispersion curves for equivalent depths of 8-90 meters; see Wheeler and Kiladis 1999 for additional details). This methodology has been demonstrated successfully in past work (e.g., Straub and Kiladis 2002; Mekonnen et al. 2008). In short, this methodology decomposes a field of data into wavenumber-frequency components for eastward moving wave disturbances.

Before the decomposition, the data is detrended and the ends of the time series were tapered to zero to control spectral leakage.

Following the methodology of Ventrice et al. (2012a,b), an index was developed by selecting all dates between June-September (JJAS) 1989 and 2009 when the minimum negative Kelvin filtered OLR anomaly (less than -1.5 standard deviations in magnitude) was over a selected grid point (10°N, 15°W). We pick the same grid point as Ventrice et al. (2012a,b) for consistency. A total of 142 CCKWs were objectively identified using this methodology. Lags were then used on this time series in order to examine propagating characteristics. For clarification, "Day 0" is when the minimum Kelvin filtered OLR anomaly moves over the selected base point.

Anomalies for all composited fields were constructed by subtracting the long-term mean and the first four harmonics of the seasonal cycle. Bootstrap random resampling tests with one thousand iterations were used for statistical significance testing on all anomalies similar to Roundy and Frank (2004). In each of these tests, a new sample equal in size to the original was randomly drawn for the original set of composite dates with replacement. The composite anomalies were considered 95% significant if 950 out of the 1000 random composites had the same sign.

All figures were made using the NCAR Command Language (NCL) version 6.0.0 (2012).

3. The influence of a convectively coupled Kelvin wave on the initiation of the pre-Alberto African easterly wave (2000)

A time-longitude plot of unfiltered TRMM 3B42 rain rate anomalies and Kelvin filtered TRMM rain rate anomalies is used to highlight the role of CCKWs on the pre-Alberto AEW (Fig. 1). The +/- 2 mm day^{-1} Kelvin filtered TRMM rain rate anomaly contour is only shown to

reference the location of strong CCKWs. ERA-Interim southerly winds at the level of the AEJ (700 hPa) are contoured black if greater than 2 ms^{-1} to indicate southerly flow associated with the circulation of AEWs. All variables were averaged over the 5-15˚N latitude band. The letter "A" represents the general time and location of the July 30th convective burst over the Darfur Mountains [20-30ºE] that has been attributed to the genesis of the pre-Alberto AEW (Berry and Thorncroft 2005). The circulation associated with the pre-Alberto AEW began one day after this convective burst (July 31). While the dynamical signature associated with the pre-Alberto AEW shows gradual intensification during its westward propagation over tropical Africa, consistent with the observations of Berry and Thorncroft (2005), its rain-rate signature reveals distinct periods of strengthening and weakening. The strengthening and weakening of the pre-Alberto AEW rain rate signature has not been discussed in previous studies and appears to be related to the passage of the convectively active and suppressed phases of consecutive eastward propagating CCKWs.

Between July 27 and August 9, two strong CCKWs are observed to propagate eastward across tropical Africa. The high resolution TRMM 3B42 product shows that the higher amplitude rain rate anomalies that occur within the convective envelopes of both CCKWs are associated with westward propagating convective signatures. In contrast to the convectively active phase, the convectively suppressed phases of both CCKWs (dashed black contours) are associated with reduced rain rate anomalies. Therefore during the analysis period, a suppressed-enhanced-suppressed-enhanced-suppressed sequence of unfiltered anomalous rain rates is clearly visible within the westward propagating MCSs over Africa. It is evident from Fig. 1 that rainfall patterns during this period over Africa were highly influenced by CCKW activity.

The anomalous rain rate signature associated with the MCS that is linked to the genesis of the pre-Alberto AEW is observed to originate on July 30 over the Darfur Mountains (~25˚E), consistent with the observations of Berry and Thorncroft (2005). The initiation of this MCS occurred roughly 15º of longitude to the east of the maximum Kelvin filtered TRMM rain rate anomaly. Past research has shown that the maximum low-level zonal wind convergence associated with CCKWs is located about 15º of longitude to the east of the center it the convective envelope (Takayabu and Murakami 1994; Straub and Kiladis 2003a,b). Therefore, this MCS developed in a region relative to the CCKW that favors for MCS development via increased low-level zonal wind convergence and vertical ascent. One day later (July 31), 700 hPa southerly winds associated with the pre-Alberto AEW circulation developed during the passage of the CCKW, indicating when the dynamical signature associated with the AEW had begun.

Between July 30 and 31, the pre-Alberto AEW was still superimposed with the convective envelope of the first CCKW. During this time, the pre-Alberto AEW had an anomalous rain rate signature greater than 40 mm day^{-1}. By August 1, the pre-Alberto AEW is collocated with the convectively suppressed phase of the CCKW. During the superposition, the anomalous rain rate signature associated with the pre-Alberto AEW weakens. Note that this convectively suppressed CCKW phase reduced rain rate anomalies to zero for other pre-existing westward moving MCSs over Africa.

The superposition between the pre-Alberto AEW and the convectively active phase of the following CCKW occurs between August 1 and 2 around 10˚W-0˚E. During this time, the anomalous rain rate signature associated with the pre-Alberto AEW increased to values greater than 40 mm day^{-1} again. At this time, Berry and Thorncroft (2005) note the merging between

low-level potential vorticity (PV) generated over the Guinea Highlands region [5-13ºN, 8-15ºW] with the pre-Alberto AEW. The low-level PV generated over the Guinea Highlands region was presumed to be generated with a coherent diurnal cycle there. Berry and Thorncroft (2005) deemed this as the final stage of an AEW life cycle and called it the "west coast development" stage. While AEWs may intensify over western tropical Africa from local processes, it is suggested that the intensification of the pre-Alberto AEW over western Africa was also in association with the superposition of the convectively active phase of an eastward propagating CCKW.

In order to investigate the initiation of the pre-Alberto AEW in greater detail, maps of CPC-merged IR (shaded) overlaid with Kelvin filtered TRMM anomalies (black contours) and ERA-interim 850 hPa wind anomalies (vectors) are constructed every six hours for the period beginning at 18Z July 29 and ending 06Z July 31 (Fig. 2). The domain of Fig. 2 is focused over eastern Africa, where the northeastern extent of the Gulf of Guinea is located in the lower left corner. At 18Z July 29, the convectively active phase of the leading CCKW is located between 0-10˚E, while its convectively-suppressed phase is located between 20-30˚E. Note that scattered MCSs were present across eastern Africa at this time, consistent with a time of day when convection is found most frequent there (Yang and Slingo 2001; Laing et al. 2008, 2011). These MCSs over eastern Africa are weaker by 00Z July 30, consistent with the diurnal cycle of convection there. By 06Z July 30, a single MCS associated with a brightness temperature value that is less than 200˚K is observed over 11˚N, 24˚E, between the convectively suppressed and active phases of the CCKW. Consistent with Fig. 1, this MCS formed roughly 15˚ of longitude to the east of the maximum positive Kelvin filtered TRMM rain rate anomaly. The MCS formed during a time of day (06Z) when convection is on average suppressed, suggesting that forcing

from the CCKW was able to overcome that associated with the coherent diurnal cycle of convection. This MCS is found to be the leading convective disturbance associated with the pre-Alberto AEW (recall Fig. 1).

By 12Z July 30, the small MCS grew in horizontal extent and magnitude during the superposition with the eastward most edge of the convectively active phase of the CCKW (Fig. 2c). Note that the scattered pre-existing MCSs over 30-40˚E weakened while superimposed with the convectively suppressed phase of the CCKW. These MCSs weakened during a time of day when convection is on average most frequent and remain in a suppressed state while superimposed with the convectively suppressed phase of the CCKW through 18Z July 30 (Fig. 2d). By 18Z July 30, the pre-Alberto MCS is now centered about 20˚E and is observed to further amplify and grow in horizontal extent while superimposed with the convectively active phase of the CCKW. Easterly wind anomalies [over 5-15ºN, 25-35ºE] are observed to the east of the convectively active phase of the CCKW, whereas westerly wind anomalies [over 5-10ºN, 0-5ºE] are observed to its west. This low-level wind signature is consistent with the low-level wind structure of the CCKW over Africa (Mounier et al. 2007). However, northerly wind anomalies are also evident within the maximum positive Kelvin filtered TRMM rain rate anomaly. These northerly wind anomalies are attributed to the formation of the low-level wind signature of the pre-Alberto AEW, not the CCKW. Further at this time, the deepest convection is collocated with the northerly flow, consistent with the observed structure of an AEW over Africa (e.g. Carlson 1969a, b; Reed et al. 1977; Duvel 1990; Diedhiou et al. 1999; Payne and McGarry 1977; Fink and Reiner 2003; Kiladis et al. 2006). By 00Z July 31, the pre-Alberto AEW has shifted slightly westward while still superimposed with western half of the convectively active phase of the CCKW (Fig 2e). A stratiform cloud signature has developed, consistent with the morphology of

cloudiness associated with a CCKW (Straub and Kiladis 2002). By 06Z July 31, deep convection associated with the AEW remained prominent while superimposed with the convectively active phase of the CCKW (Fig. 2f). This deep convection remained active during a time of day when convection is on average suppressed, suggesting that the combined forcing from the CCKW and the newly spawned AEW is greater than that of the forcing from the coherent diurnal cycle of convection over Africa.

Each phase of the CCKW acts oppositely to either increase or reduce rainfall over tropical Africa (e.g., Mounier et al 2007; Laing et al. 2011). The convectively active phase of the CCKW increases the amplitude and frequency of westward moving MCSs, whereas the suppressed phase reduces both. In the pre-Alberto AEW case, the convectively suppressed phase of the leading CCKW may have contributed to the decay of the MCS on July 29 that Hill and Lin (2003) argue was important for the pre-Alberto AEW genesis over the Ethiopia Highlands (recall Fig. 1). The initiation of the MCS that Berry and Thorncroft (2005) argue later developed into the pre-Alberto AEW has been shown to occur during the passage of the convectively active phase of an eastward propagating CCKW. This MCS amplified within the convectively active phase of the CCKW during a time of day when convection is expected to be active. However, this MCS also remained prominent while superimposed with the convectively active phase of the CCKW through 06Z, a time of day where convection is on average suppressed over Darfur. A study comparing CCKWs and the diurnal cycle of convection within the tropics is needed to fully understand the role of the CCKW and diurnally varying convection but is beyond the scope of this study. Motivated by the results above, we now explore the climatological influence of CCKWs over tropical Africa in order to better understand the physical reasons of why the pre-Alberto AEW initiated during the passage of the CCKW.

4. The climatological role of the convectively coupled Kelvin waves on the synoptic environment over Africa

The composite zonal wind anomaly structure of a CCKW is observed to have strong westward tilts in the lower troposphere, with upper-tropospheric winds generally opposite to those in the lower-troposphere (e.g., Straub and Kiladis 2002; Kiladis et al. 2009; Ventrice et al. 2012b). Because of this vertical wind structure, CCKWs must influence the background low-level easterly vertical wind shear over tropical Africa during boreal summer. For example, the amplification of low-level easterly vertical wind shear over Africa could provide a favorable environment for the development of organized convection (e.g., Rotunno et al. 1988; Lafore and Moncrieff 1989). Further, since CCKWs strongly impact the zonal wind in the lower troposphere, CCKWs might also alter the nature of the mid-level AEJ. These parameters are now explored in turn to investigate the role of CCKWs on the synoptic environment important for convection and AEW growth over Africa.

i) 925-700 hPa Vertical Wind Shear

The organization of ordinary convection into propagating MCSs is favored under moderate vertical wind shear of the horizontal wind (e.g., Rotunno et al. 1988; Lafore and Moncrieff 1989). Over Africa, Laing et al. (2008, 2011) found that frequent deep convection is associated with maxima in the 925-600 hPa easterly shear over northern tropical Africa during May to August. This low-level vertical wind shear varies day-to-day and is composed by the low-level monsoon westerlies and the mid-level AEJ. Since CCKWs are characterized by strong westward vertical tilts with height of the zonal wind, both the 925 hPa and 700 hPa zonal wind fields are strongly influenced by CCKW passages. Therefore, these waves must affect the low-level vertical wind shear over Africa.

Anomalies of 925-700 hPa vertical wind shear magnitude (shaded) and direction (vectors) are averaged over each lag of the CCKW index to investigate the influence of the CCKW on low-level shear over Africa (Fig. 3). The direction of shear represents the vector difference between 925 hPa and 700 hPa. On Day -1, the convectively suppressed phase of the CCKW is located over western tropical Africa, while its convectively active phase is located over the eastern tropical Atlantic (Fig. 3a). Anomalous easterly shear extends from the western half of the convectively suppressed phase of the CCKW through the convectively active phase, covering over 30˚ of longitude. This anomalous easterly shear adds 0.5-1 ms^{-1} to the background easterly shear over Africa. Northeast of the convectively suppressed phase of the CCKW is a small area of anomalous westerly shear. The anomalous westerly shear is created by anomalous low-level (850 hPa and below) easterly flow associated with the convectively suppressed phase of the CCKW, where easterly anomalies weaken above 850 hPa. This anomalous westerly shear is collocated with the convectively suppressed phase of the CCKW and reduces the background low-level easterly vertical wind shear over Africa during the next two days (Fig. 3b,c).

By Day 0, the convectively active phase of the CCKW is located over the coast of West Africa (Fig. 3b). Easterly vertical wind is collocated with the convectively active phase of the CCKW and is associated with an increase to the background easterly vertical wind shear there. In addition to occurring within the convectively active phase of the CCKW, significant anomalous easterly shear extends eastward to the maximum positive Kelvin filtered OLR anomaly. The eastward extension of increased low-level easterly shear suggests that the area in between the leading suppressed phase and the convectively active phase of the CCKW is also an environment that favors for the development of organized convection. A vertical cross section of anomalous

zonal wind on Day 0 over the longitude of 8.5ºN shows that the increased easterly vertical wind shear in between the leading convectively suppressed phase and the active phase of the CCKW (0º-10ºW) is primarily driven by anomalous easterly winds extending back towards the west with height (Fig. 4). The anomalous easterly shear within the convectively active phase of the CCKW (0º-25ºW) is from the combination of mid-tropospheric easterly flow undercut by anomalous westerly flow.

Between Day +1 and Day +4, anomalous easterly vertical wind shear progresses eastward with the convectively active phase of the CCKW (Fig. 3c-f). Following this convectively active phase of the CCKW is its suppressed phase, which is associated with anomalous westerly vertical wind shear. Between Day +1 and Day +4, this anomalous westerly vertical wind shear reduces the background easterly vertical wind shear over the equatorial Atlantic and Africa by roughly 0.5 ms^{-1} (Fig. 3c-f).

By increasing the background low-level easterly vertical wind shear over Africa, the CCKW provides an environment favorable for developing MCSs. The more frequent, stronger MCSs within the convective envelope of the CCKW also increases the likelihood of initiating or intensifying a pre-existing AEW. This increased vertical wind shear is observed to occur within the convectively active phase of the CCKW, but increased vertical wind shear also occurs just ahead of it. Recall that the MCS that later developed into the pre-Alberto AEW formed in between the leading convectively suppressed phase and convectively active phase of a CCKW (Fig. 2c). This MCS flourished during the passage of the convectively active phase of the CCKW, consistent with the increased low-level easterly vertical low-level wind shear generated by the CCKW.

ii) The impact of convectively coupled Kelvin waves on the horizontal structure of the African easterly jet

Fields of total 700 hPa easterly winds (dashed contours), anomalies of 700 hPa zonal wind (shaded), and Kelvin filtered OLR anomalies (bold contours) are averaged over each lag of the CCKW index to investigate the impact of the CCKW passage on the horizontal structure of the AEJ (Fig. 5). Easterly 700 hPa wind anomalies (shaded) generally occur within the leading convectively suppressed phase of the CCKW (see Fig. 4). These easterly anomalies also extend westward through the eastward most edge of the convectively active phase, consistent with the westward vertical tilted structure of the CCKW. Anomalous westerly winds are observed to follow the minimum negative Kelvin filtered OLR anomaly of the CCKW (Fig. 5d-l). These anomalous westerly winds extend westward through the following convectively suppressed phase of the CCKW (Fig. 5h-i). It is important to comment on the anomalous easterly wind signature over the Atlantic between Day -4 and Day -2 (Fig. 5c-e). During this time, there are easterly anomalies collocated within the convectively active phase of the CCKW. This signature is not representative of the expected structure of the CCKW and is associated with an interference pattern caused by a westward moving signature that has been attributed to a Saharan air layer (SAL) outbreak across the tropical Atlantic between Day -6 and Day 0 (Ventrice et al. 2012b).

The AEJ can be modulated by the CCKW in two processes. The first process is associated with the equatorial wind structure of the CCKW, which can modulate the horizontal shear of the AEJ on the equatorward side. The second process is associated with convection generated by the CCKW over Africa. Following the argument of Thorncroft and Blackburn (1999), increased convection on the equatorward side of the jet generates PV near the level of the

jet, acting to strengthen the jet. For this analysis, we only focus on the first process. Keeping these principles in mind, we begin our analysis when the convectively suppressed phase of the CCKW is located over the tropical Atlantic on Day -6.

On Day -6, the highest amplitude easterly winds associated with the AEJ are located over West Africa and centered over the coast of West Africa, indicated by the -9 ms^{-1} isotach (Fig. 5a). Between Day -5 and Day -2, the -9 ms^{-1} isotach extends westward over the central tropical Atlantic (to ~40˚W), highlighting a westward extension of the AEJ (5ig. 4b-e). This westward extension of the jet over the tropical Atlantic separates moist monsoonal air equatorward of the jet, and a dry SAL poleward of it. Consistent with these observations, Ventrice et al. (2012b) found that an area of anomalously dry air progressed westward across the northern tropical Atlantic during the passage of the convectively active phase of a CCKW.

Over Africa, the 700 hPa easterly wind anomalies associated with the convectively suppressed phase of the CCKW increase the total magnitude of the AEJ between Day -4 and Day +1 (Fig. 5c-h). Between Day -1 and Day +1, Kelvin wave induced easterly anomalies accelerate the upstream half of the AEJ, extending the jet entrance region eastward over the Darfur Mountains. Previous literature that has focused on the intraseasonal variability of AEW activity (e.g., Leroux et al. 2010; Ventrice et al. 2011; Alaka and Maloney 2012) have shown that an eastward extension of the AEJ entrance region over the Darfur Mountains precedes a period of increased AEW activity. The eastward extension of the AEJ entrance region will tend to increase barotropic and baroclinic energy conversions for AEW growth over the Darfur Mountains and Ethiopian Highlands. Therefore, the convectively suppressed phase of the CCKW is modifying the upstream half of the AEJ to pre-condition, or “load” the jet for a future period of increased AEW activity. These easterly wind anomalies are present for about four days and so whether

these exist long enough to influence the subsequent AEW activity is an open question that should be investigated in future work.

For all days in Fig. 5, the maximum zonal wind anomaly is generally peaked equatorward of the AEJ. This signature suggests that the CCKW is affecting the horizontal shear across the AEJ, which modifies the relative vorticity sign-reversal in the jet core. A tighter horizontal gradient of easterly zonal wind is indicative of a more unstable AEJ, and vice versa. Focusing on the convectively suppressed phase of the CCKW, the anomalous easterly winds equatorward of the AEJ reduce the horizontal meridional gradient of zonal wind and suggests that the jet is more stable, even though the jet core is strongest during this period. Therefore, the AEJ is less unstable over Africa between Day -2 and Day 0. The westerly winds associated with the convectively active phase of the CCKW increase horizontal shear on the equatorward side of the AEJ over Africa. This suggests that the AEJ is more unstable during the passage of the convectively active phase of the CCKW, which favors for AEW initiation and growth over Africa between Day +1 and Day +5.

iii) 2-10 day filtered Eddy Kinetic Energy

We hypothesize that the passage of the convectively active phase of the CCKW will increase AEW activity over Africa (Fig. 1, Mekonnen et al. 2008). First, the leading convectively suppressed phase of the CCKW extends and accelerates the AEJ over the Darfur Mountains (the trigger region). This mechanism acts to "load" the AEJ over the Darfur Mountains and Ethiopian Highlands. Then more frequent strong and long lasting MCSs initiate within the convective envelope of the CCKW (e.g., Mounier et al. 2007; Laing et al. 2011). These MCSs thrive in an environment characterized by increased low-level easterly shear. Therefore, these MCSs are hypothesized to convectively trigger AEWs.

A time-longitude composite of 2-10 day filtered EKE anomalies averaged over each lag of the CCKW index shows the relationship between CCKWs and AEW activity (Fig. 6). Recall that Day 0 is when the minimum Kelvin filtered OLR anomaly is located over the base point (10˚N, 15˚W). Between Day -5 and Day +2, no significant positive EKE anomalies develop over the tropical Atlantic during the passage of the convectively active phase of the CCKW. Positive EKE anomalies first develop over West Africa (15˚W-0˚E) after the passage of the convectively active phase of the CCKW over West Africa. This result suggests that the convectively active phase of the CCKW is insufficient alone to modulate easterly wave activity without the presence of the AEJ and African topography. Positive EKE anomalies progress eastward with the convective envelope of the CCKW to roughly 0˚E. Thereafter, this large area of positive EKE anomalies over West Africa is observed to progress westward over the Atlantic with an average phase speed of 9.0 m s^{-1}, consistent with the phase speed of an AEW (e.g., Kiladis et al. 2006, and references therein). This anomalous EKE signature is composed of many instances where pre-existing AEWs are becoming stronger after the passage of the convectively active phase of the CCKW (not shown), similar to the pre-Alberto case in 2000 and the pre-Debby AEW case in 2006 (Ventrice et al. 2012a).

There are three distinct peaks of significant positive EKE anomalies over the tropical Atlantic between Day +2 and Day +5. This is suggestive of that fact that topography in West Africa is acting to influence the spawning or intensification locations of AEWs after the passage of the convectively active phase of the CCKW. The extent to which AEWs are being triggered or enhanced over the Guinea Highlands region [5-13ºN, 8-15ºW] would need to be investigated in a more detailed analysis. Further, the three significant peaks of AEW activity over the tropical Atlantic confirms the observations of Ventrice et al. (2012b) that the wave-like disturbance over

the tropical Atlantic that develops after the passage of the convectively active phase of the CCKW is a train of AEWs. Ventrice et al. (2012b) found that this train of AEWs developed after a zonally oriented strip of low-level cyclonic relative vorticity was generated after the passage of the convectively active phase of the composited CCKW over western tropical Africa (see their Fig. 7).

Positive EKE anomalies develop over the Darfur Mountains (25˚E) and over and downstream of the Ethiopian Highlands (30-35˚E) during the passage of the eastern most edge of the convectively active phase of the CCKW between Day +2 and Day +3. Recall that the wind signature associated with the pre-Alberto AEW formed within the convectively active phase of the CCKW over the Darfur Mountains (Fig. 1). The positive EKE anomalies generated over the Darfur Mountains amplify within the convectively active phase of the CCKW and progress westward on time scales consistent with AEWs directly after the passage. This area of positive EKE anomalies is observed to progress westward across tropical Africa between Day +6 and Day +10 and over the tropical Atlantic thereafter.

Interestingly on Day -1, significant positive EKE anomalies are generated over 20-30˚E prior to and during the passage of the convectively suppressed phase of the CCKW. Recall that this is when the entrance region of the AEJ extends eastward over eastern highlands of Africa (Fig. 5f). Therefore, any diurnally driven MCSs generated over the Darfur Mountains and Ethiopian Highlands prior to the passage of the convectively suppressed phase of the CCKW over might be sufficient enough to trigger an AEW due to the increased barotropic and baroclinic energy conversions associated with the eastward shifted jet. Further work is needed on the role of CCKWs and the eastward shifted AEJ over the eastern African highlands and their combined impact on AEW activity.

5. Discussion and Conclusions

This study shows evidence that CCKWs modulate AEW activity on synoptic timescales over West Africa during boreal summer. A TRMM 3B42 rain-rate anomaly time-longitude plot showed that the initiation of the pre-Alberto AEW (2000) occurred during the passage of a CCKW (Fig. 1). The convection attributed to the genesis of the pre-Alberto AEW described by Berry and Thorncroft (2005) was likely triggered by the passage of an eastward propagating CCKW. It has been shown that a series of consecutive CCKWs strongly influenced the pre-Alberto AEW over Africa. We have also shown that the initiation and west coast developing stages (e.g., Berry and Thorncroft 2005) of the pre-Alberto AEW were times when the pre-Alberto AEW was superposed with a convectively active phase of a CCKW.

The convectively active phase of CCKWs modulates the synoptic environment over tropical Africa through convective and dynamical processes that provides a favorable environment for initiating and amplifying MCSs. Figure 7(a,b) shows two schematic diagrams characterizing the evolution of the environment over Africa during the passage of a CCKW over West Africa at arbitrary times t = 0 (when the active phase of the CCKW is over the Guinea Highlands) and t = t + 3 days (when the active phase of the CCKW is over the eastern African highlands). Beginning with time t = 0, the convectively active phase of the CCKW is located over the Guinea Highlands region in West Africa (7a). Enhanced low-level easterly shear (purple arrow) extends from the convective envelope of the CCKW eastward to the center of its convectively suppressed phase, with anomalous low-level westerly shear ahead of this convectively suppressed phase. Since the low-level shear is climatologically easterly over Africa and is attributed to the combination of the mid-level AEJ and low-level monsoon westerlies, the Kelvin-induced low-level westerly shear that occurs just the east of the leading suppressed phase

of the CCKW reduces the background low-level easterly vertical wind shear. In contrast, the Kelvin-induced low-level easterly shear that occurs within and immediately to the east of the convectively active phase of the CCKW increases the background low-level easterly shear over Africa. This increased anomalous easterly shear generated by the CCKW is beneficial for strong and long-lasting MCS development (e.g., Mounier et al. 2007; Laing et al. 2011). By increasing the frequency of strong, long-lasting MCSs, the CCKW increases the number of convective triggers over Africa that is suggested to be important for AEW initiation over the eastern African highlands (e.g., Thorncroft et al. 2008).

The AEJ (red dashed line) becomes more unstable (thick dark-red dashed line) over western Africa during the passage of the convectively active phase of the CCKW. Anomalous westerly flow at the level of the AEJ associated with the CCKW imposes horizontal shear on the AEJ, which increases the meridional gradient of zonal wind at the level of the jet. The strengthening of the meridional gradient of zonal wind suggests that the negative gradient of potential vorticity at the level of the jet is becoming more negative (not shown), indicative of a more unstable jet. The more unstable jet is consistent with the observed enhanced AEW activity (e.g., Leroux and Hall 2009). Further, the entrance region of the AEJ extends eastward over the eastern African highlands. The eastward extension of AEJ has been found to precede a period of enhanced AEW activity (e.g., Leroux et al. 2011; Ventrice et al. 2011; Alaka and Maloney 2012). Since the CCKW provides an environment favorable for strong convection that can grow along a more unstable AEJ, a westward propagating AEW activity response (orange slanted line) develops just after the passage of the convectively active phase of the CCKW over the Guinea Highlands region.

At a slightly later time (t + 3 days), the convective envelope associated with the CCKW is located over eastern African highlands (7b). Enhanced low-level easterly shear propagates eastward with the CCKW, now providing a favorable environment for organized convection over the eastern African highlands. Westerly wind anomalies at the level of the AEJ extend westward from the convectively active phase of the CCKW, imposing horizontal shear on the AEJ over a larger region of Africa. Therefore, the AEJ is more unstable over a large horizontal extent for AEW growth. Consistent with the environment favorable for AEW initiation and growth, a new AEW response develops over the eastern African highlands during the passage of the convectively active phase of the CCKW. The AEW response to the CCKW passage over the Guinea Highlands region at time t = 0 has propagated back towards the west over the tropical Atlantic and become important for Atlantic tropical cyclogenesis (e.g., Ventrice et al. 2012a.b).

An issue that needs to be addressed in future work is whether the eastward extension of the AEJ over the eastern African highlands could be sufficient enough for AEW genesis even though there is local suppression forced by the CCKW. Further, is the sub-weekly period that the AEJ becomes more unstable in association with the passage of the convectively active phase of the CCKW long enough to aid in an extended period of enhanced AEW activity? Or does the common phasing with a lower frequency mode, such as the Madden Julian Oscillation (MJO) become important to consider (e.g., Ventrice et al. 2012b)? Such questions should be further studied using observations and models to better understand the variability of AEWs and MCSs in support of operational forecasting at daily to intraseasonal timescales.

In addition to boreal spring (e.g., Nguyen and Duvel 2009), CCKWs impact African weather variability during boreal summer. African forecasters should be aware of CCKWs for the direct impact on rainfall, as well as the triggering of AEWs over the Darfur Mountains, the

Ethiopian Highlands, and even possibly the Guinean Highlands where east Atlantic tropical cyclogenesis implications become important to consider.

Acknowledgements. The authors would like thank NOAA CPC, NCEP, and the NASA TRMM program for providing the satellite data in the study. We extend our gratitude to NASA for the Grant NNX09AD08G which supported this research. Interpolated OLR data were provided by the NOAA/OAR/ESRL PSD, Boulder, Colorado, USA, from their web site at http://www.esrl.noaa.gov/psd/. We also would like to thank NCL for their support in generating the figures used in this manuscript.

References:

Alaka, G. J., and E. D. Maloney, 2012: The influence of the MJO on upstream precursors to African easterly waves. *J. Climate*, *early online release.*

Avila, L.A. and R.J. Pasch, 1992: Atlantic tropical systems of 1991. *Mon. Wea. Rev.*, **120**, 2688-2696.

Berry, G., and C.D. Thorncroft, 2005: Case study of an intense African easterly wave. *Mon. Wea. Rev.,* **133**, 752–766.

Carlson, T. N., 1969a: Synoptic histories of three African disturbances that developed into Atlantic hurricanes. *Mon. Wea. Rev*., **97**, 256–276.

——, 1969b: Some remarks on African disturbances and their progress over the tropical Atlantic. *Mon. Wea. Rev*., **97**, 716–726.

Diedhiou, A., S. Janicot, S. Viltard, and H. Laurent, 1999: Easterly wave regimes and associated convection over West Africa and the tropical Atlantic: Results from NCEP/NCAR and ECMWF reanalyses. *Climate Dyn.,* **15**, 795–822.

Duvel, J. P., 1990: Convection over tropical Africa and the Atlantic Ocean during northern summer. Part II: Modulation by easterly waves. *Mon. Wea. Rev.,* **118**, 1855–1868.

Frank, N. L., 1970: Atlantic tropical systems of 1969. *Mon. Wea. Rev.*, **98**, 307–314.

Fink, A. H., and A. Reiner, 2003: Spatio-temporal variability of the relation between African Easterly waves and West African squall lines in 1998 and 1999. *J. Geophys. Res.*, **108**, 4332

Gruber, A., 1974: The wavenumber-frequency spectra of satellite-measured brightness in the tropics. *J. Atmos. Sci.*, **31**, 1675-1680.

Hall, N. M. J., G. N. Kiladis, and C. D. Thorncroft, 2006: Three dimensional structure of African easterly waves. Part II: Dynamical modes. *J. Atmos. Sci.,* **63**, 2231–2245.

Hill, C. M., and Y-L. Lin, 2003: Initiation of a mesoscale convective complex over the Ethiopian highlands preceding the genesis of Hurricane Alberto (2000): A precursor to tropical cyclogenesis. *Geophys. Res. Lett.*, **30**, 1232, doi:10.1029/2002GL016655.

Hsieh, J.-H., and K. H. Cook, 2005: Generation of African easterly wave disturbances: Relationship to the African easterly jet. *Mon. Wea. Rev.*, **133**, 1311–1327.

Huffman, G. J., and Coauthors, 2007: The TRMM Multisatellite Precipitation Analysis (TMPA): Quasi-global, multiyear, combined-sensor precipitation estimates at fine scales. *J. Hydrometeor*., **8**, 38–55.

Kiladis, G. N., C. D. Thorncroft, and N. M. J. Hall, 2006: Three dimensional structure and dynamics of African easterly waves. Part I: Observations. *J. Atmos. Sci.*, **63**, 2212–2230.

——, M.C. Wheeler, P.T. Haertel, K. H. Straub, and P. E. Roundy, 2009: Convectively coupled equatorial waves. *Rev. Geophys.*, **47**, RG2003, doi:10.1029/2008RG000266.

Lafore, J.-P., and M. W. Moncrieff, 1989: a numerical investigation of the organization and interactions of the convective and stratiform regions of tropical squall lines. *J. Atmos. Sci.*, **46**, 521-544.

Laing, A. G., R.E. Carbone, V. Levizzani, and J. D. Tuttle, 2008: The propagation and diurnal cycles of deep convection in northern tropical Africa. *Quart. J. Roy. Meteor. Soc.,* **134,** 93–109.

——, ——, ——, 2011: Cycles and propagation of deep convection over equatorial Africa. *Mon. Wea. Rev.*, **139**, 2832-2853.

Leroux, S., and N. M. Hall, 2009: On the relationship between African easterly waves and the African easterly jet. *J. Atmos. Sci.*, **66**, 2303–2316.

——, ——, and G. N. Kiladis, 2010: A climatological study of transient–mean-flow interactions over West Africa. *Quart. J. Roy. Meteor. Soc.*, **136**, 397–410.

——, ——, ——, 2011: Intermittent African easterly wave activity in a dry atmospheric model: Influence of the extratropics. *J. Climate*, **24**, 5378-5396.

Liebmann, B., and C. A. Smith, 1996: Description of a complete (interpolated) outgoing long-wave radiation dataset. *Bull. Amer. Meteor. Soc.*, **77**, 1275–1277.

Lin, H., G. Brunet, and J. Derome, 2007: Intraseasonal variability in a dry atmospheric model. *J. Atmos. Sci.*, **64**, 2422-2441.

Mekonnen, A., C.D. Thorncroft and A.R. Aiyyer, 2006: Analysis of convection and its association with African easterly waves. *J. Climate,* **19**, 5405-5421.

——, C.D. Thorncroft, A.R. Aiyyer, G.N. Kiladis, 2008: Convectively coupled Kelvin waves over tropical Africa during the boreal summer: structure and variability. *J. Climate,* **21**, 6649-6667.

Mounier, F., G. N. Kiladis, and S. Janicot, 2007: Analysis of the dominant mode of convectively coupled Kelvin waves in the West African monsoon. *J. Climate,* **20**, 1487–1503.

Nguyen, H. and J. P. Duvel, 2008: Synoptic Wave Perturbations and Convective Systems over Equatorial Africa. *J. Climate*, **23**, 6372-6388.

Payne, S. W., and M. M. McGarry, 1977: The relationship of satellite inferred convective activity to easterly waves over West Africa and the adjacent ocean during phase III of GATE. *Mon. Wea. Rev.,* **105**, 414–420.

Pires, P. J-L. Redelsperger, J-P. Lafore, 1997: Equatorial atmospheric waves and their association to convection. *Mon. Rev. Rev.*, **125**, 1167-1184.

Reed, J. R., D. C. Norquist, and E. E. Recker, 1977: The structure and properties of African wave disturbances as observed during phase III of GATE. *Mon. Wea. Rev.*, **105**, 317-333.

Rennick, M. A., 1976: The generation of African waves. *J. Atmos. Sci.*, **33**, 1955-1969.

Roundy, P. E., and W. M. Frank, 2004: A climatology of waves in the equatorial region, *J. Atmos. Sci.*, **61**, 2105–2132.

Rotunno, R., J. B. Klemp, and M. L. Weisman, 1988: A theory for strong, long-lived squall lines. *J. Atmos. Sci.,* **45**, 463-485.

Schreck, C. J. III, and J. Molinari, 2011: Tropical cyclogenesis associated with Kelvin waves and the Madden-Julian Oscillation. *Mon. Wea. Rev.*, **139**, 2723-2734.

Simmons, A. J., 1977: A note on the instability of the African easterly jet. *J. Atmos. Sci.*, **34**, 1670–1674.

——, S. Uppala, D. Dee, and S. Kobayashi, 2007: ERA Interim: New ECMWF

reanalysis products from 1989 onwards. ECMWF Newsletter, No. 110, ECMWF, Reading, United Kingdom, 25–35.

Straub, K. H., and G. N. Kiladis, 2002: Observations of a convectively coupled Kelvin waves in the eastern Pacific ITCZ. *J. Atmos. Sci.,* **59,** 30–53.

——, and ——, 2003a: Extratropical forcing of convectively coupled Kelvin waves during austral winter. *J. Atmos. Sci.,* **60**, 526–543.

——, and ——, 2003b: The Observed Structure of Convectively Coupled Kelvin Waves: Comparison with Simple Models of Coupled Wave Instability. *J. Atmos. Sci.*, **60**, 1655-1668.

Takayabu, Y. N., 1991: The structure of super cloud clusters observed in 1–20 June 1986 and their relationship to easterly waves. *J. Meteor. Soc. Japan,* **69,** 105–125.

——, and M. Murakami, 1994: Large-scale cloud disturbances associated with equatorial waves. Part I: Spectral features of the cloud disturbances. *J. Meteor. Soc. Japan,* **72**, 433–448.

The NCAR Command Language (Version 6.0.0) [Software]. (2012). Boulder, Colorado: UCAR/NCAR/CISL/VETS. http://dx.doi.org/10.5065/D6WD3XH5.

Thompson, R. M., Jr., S. W. Payne, E. E. Recker, and R. J. Reed, 1979: Structure and properties of synoptic-scale wave disturbances in the Intertropical Convergence Zone of the eastern Atlantic. *J. Atmos. Sci.,* **36**, 53–72.

Thorncroft, C. D., and B. J. Hoskins, 1994a: An idealized study of African easterly waves. Part I: A linear view. *Quart. J. Roy. Meteor. Soc.,* **120**, 953–982.

——, and ——, 1994b: An idealized study of African easterly waves. Part II: A non linear view. *Quart. J. Roy. Meteor. Soc.*, **120**, 983–1015.

——, and M. Blackburn, 1999: Maintenance of the African easterly jet. *Quart. J. Roy. Meteor. Soc.*, **125**, 763–786.

——, N. M. Hall, and G. K. Kiladis, 2008: Three-dimensional structure and dynamics of African easterly waves. Part III: genesis. *J. Atmos. Sci.*, **65**, 3596-3607.

Ventrice, M. J., C. D. Thorncroft, and P. E. Roundy, 2011: The Madden Julian's Oscillation on African easterly waves and downstream tropical cyclogenesis. *Mon. Wea. Rev.*, **139**, 2704-2722.

——, ——, and M. A. Janiga, 2012a: Atlantic tropical cyclogenesis: A three-way interaction between an African easterly wave, diurnally varying convection, and a convectively-coupled atmospheric Kelvin wave. *Mon. Wea. Rev.*, **140**, 1108-1124.

——, ——, and Carl. J. Schreck, 2012b: Impacts of convectively coupled Kelvin waves on environmental conditions associated with Atlantic tropical cyclogenesis, *Mon. Wea. Rev.*., in press.

Wheeler, M., and G. N. Kiladis, 1999: Convectively coupled equatorial waves: Analysis of clouds and temperature in the wavenumber– frequency domain. *J. Atmos. Sci.*, **56**, 374–399.

——, ——, and P. J. Webster, 2000: Large-scale dynamical fields associated with convectively coupled equatorial waves. *J. Atmos. Sci.*, **57**, 613–640.

Zangvil, A., 1975: Temporal and spatial behavior of large-scale disturbances in tropical cloudiness deduced from satellite brightness data. *Mon. Wea. Rev.*, **103**, 904-920.

Figures:

FIG. 1. A time-longitude plot of unfiltered TRMM 3B42 rain-rate anomalies (positive anomalies shaded only) overlaid with Kelvin filtered TRMM anomalies (contoured) averaged between the 5-15˚N band for the period of July 20-August 10, 2000. The initiation of the MCS linked to the genesis of the pre-Alberto AEW is denoted as the letter "A". The +/- 2 mm day^{-1} Kelvin filtered TRMM anomaly is only contoured to indicate each phase of the CCKW. Positive values of ECWMF-interim total meridional wind is contoured (black); contouring begins at 2 ms^{-1}; contour interval is 1 ms^{-1}.

FIG. 2. CPC-merged IR (shaded) overlaid with Kelvin filtered TRMM rain rate anomalies (black contours) and ERA-Interim 850 hPa wind anomalies (vectors) for the period beginning at 18Z July 29, 2000 and ending 06Z July 31, 2000. Shade interval is 2.5˚K; contours interval is 0.2 mm day^{-1}; reference vector is 10 ms^{-1}.

FIG. 3. The 925-700 hPa vertical wind shear vector and magnitude (shaded) anomaly composite averaged over each CCKW lag. Wind shear magnitude anomalies statistically different than zero at the 90% level are shaded. Vectors represent the vector difference between 925 hPa and 700 hPa. Kelvin filtered OLR anomalies are contoured if statistically different than zero at the 95% level. Negative Kelvin filtered OLR anomalies are dashed. Shade interval is 0.1 ms^{-1}; contour interval is 3 Wm^{-2}; reference shear vector is 0.5 ms^{-1}.

FIG. 4. A height-longitude composite of zonal wind anomalies along 8˚N on Day 0 of the CCKW index. The slanted black line-on-white fill represents the topography of West Africa.

FIG. 5. 700 hPa zonal wind anomalies averaged over each CCKW lag. Anomalies statistically significantly different than zero at the 95% level are shaded. Total raw easterly zonal wind is composited for each CCKW lag and contoured. Kelvin filtered OLR anomalies are contoured (bold). Shade interval is 0.2 ms^{-1}; Kelvin filtered OLR contour interval is 3 Wm^{-2}; easterly 700 hPa winds contour range is from -10 to -4 ms^{-1}; wind contour interval is 1 ms^{-1}. The red dashed contour highlights the -9 ms^{-1} contour.

FIG. 6. A time-longitude composite of 2-10 day filtered 700 hPa eddy kinetic energy (shaded) averaged and over each lag of the CCKW index between the 7.5-15˚N band. Positive (Negative) eddy kinetic energy anomalies statistically different than zero at the 90% level are within the solid (dashed) contour. Kelvin filtered OLR anomalies are averaged over the 5-10˚N latitude band and are boldly contoured. Negative Kelvin filtered OLR anomalies are dashed. Shade interval is 0.1 m^2s^{-2}; contour interval is 3 Wm^{-2}.

FIG. 7. A schematic diagram representing the modulation of the African environment and AEW activity by the passage of a CCKW when the convective envelope of the CCKW is over (a) the Guinea Highlands and (b) approximately three days later when it is over the eastern African highlands.

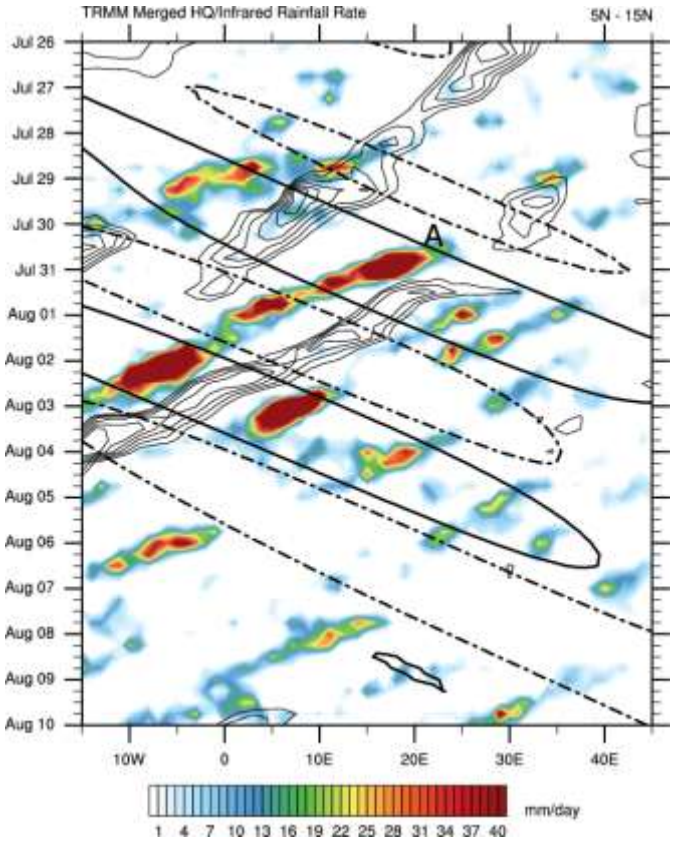

FIG. 1. A time-longitude plot of unfiltered TRMM 3B42 rain-rate anomalies (positive anomalies shaded only) overlaid with Kelvin filtered TRMM anomalies (contoured) averaged between the 5-15˚N band for the period of July 26-August 10, 2000. The initiation of the MCS linked to the genesis of the pre-Alberto AEW is denoted as the letter "A". The +/- 2 mm day^{-1} Kelvin filtered TRMM anomaly is only contoured to indicate each phase of the CCKW. Positive values of ECWMF-interim total meridional wind is contoured (black); contouring begins at 2 ms^{-1}; contour interval is 1 ms^{-1}.

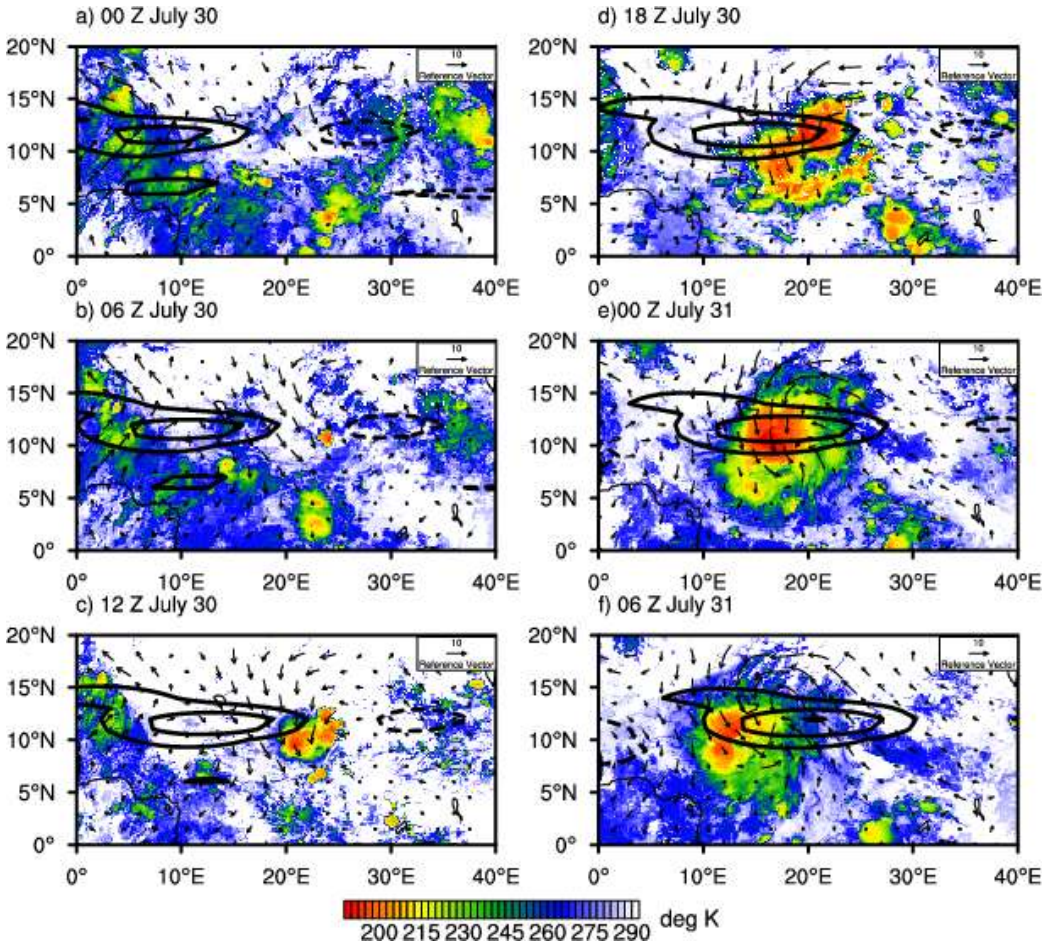

FIG. 2. CPC-merged IR (shaded) overlaid with Kelvin filtered TRMM rain rate anomalies (black contours) and ERA-Interim 850 hPa wind anomalies (vectors) for the period beginning at 00Z July 30, 2000 and ending 06Z July 31, 2000. Shade interval is 2.5˚K; contours interval is 0.2 mm day^{-1}; reference vector is 10 ms^{-1}.

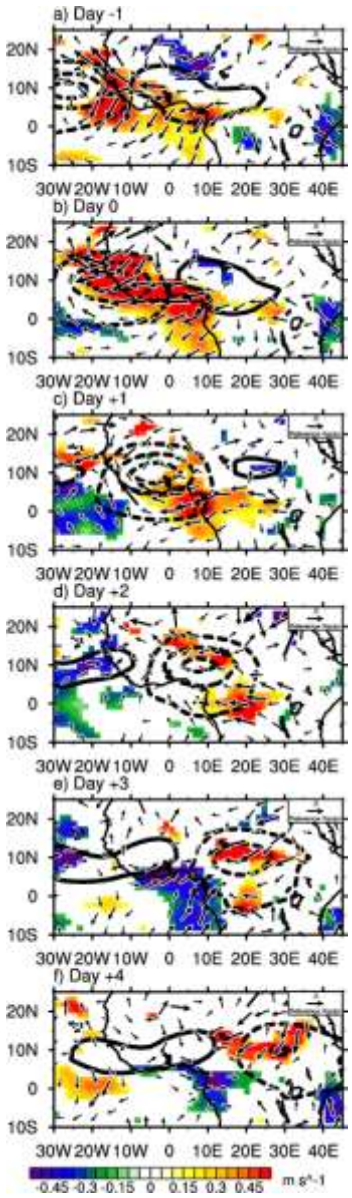

FIG. 3. The 925-700 hPa vertical wind shear vector and magnitude (shaded) anomaly composite averaged over each CCKW lag. Wind shear magnitude anomalies statistically different than zero at the 90% level are shaded. Vectors represent the vector difference between 925 hPa and 700 hPa. Kelvin filtered OLR anomalies are contoured if statistically different than zero at the 95% level. Negative Kelvin filtered OLR anomalies are dashed. Shade interval is 0.1 ms^{-1}; contour interval is 3 Wm^{-2}; reference shear vector is 0.5 ms^{-1}.

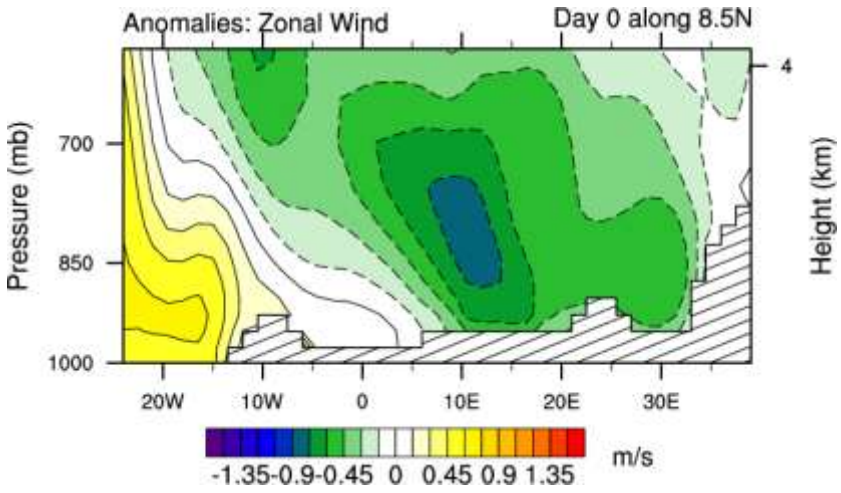

FIG. 4. A height-longitude composite of zonal wind anomalies along 8˚N on Day 0 of the CCKW index. The slanted black line-on-white fill represents the topography of West Africa.

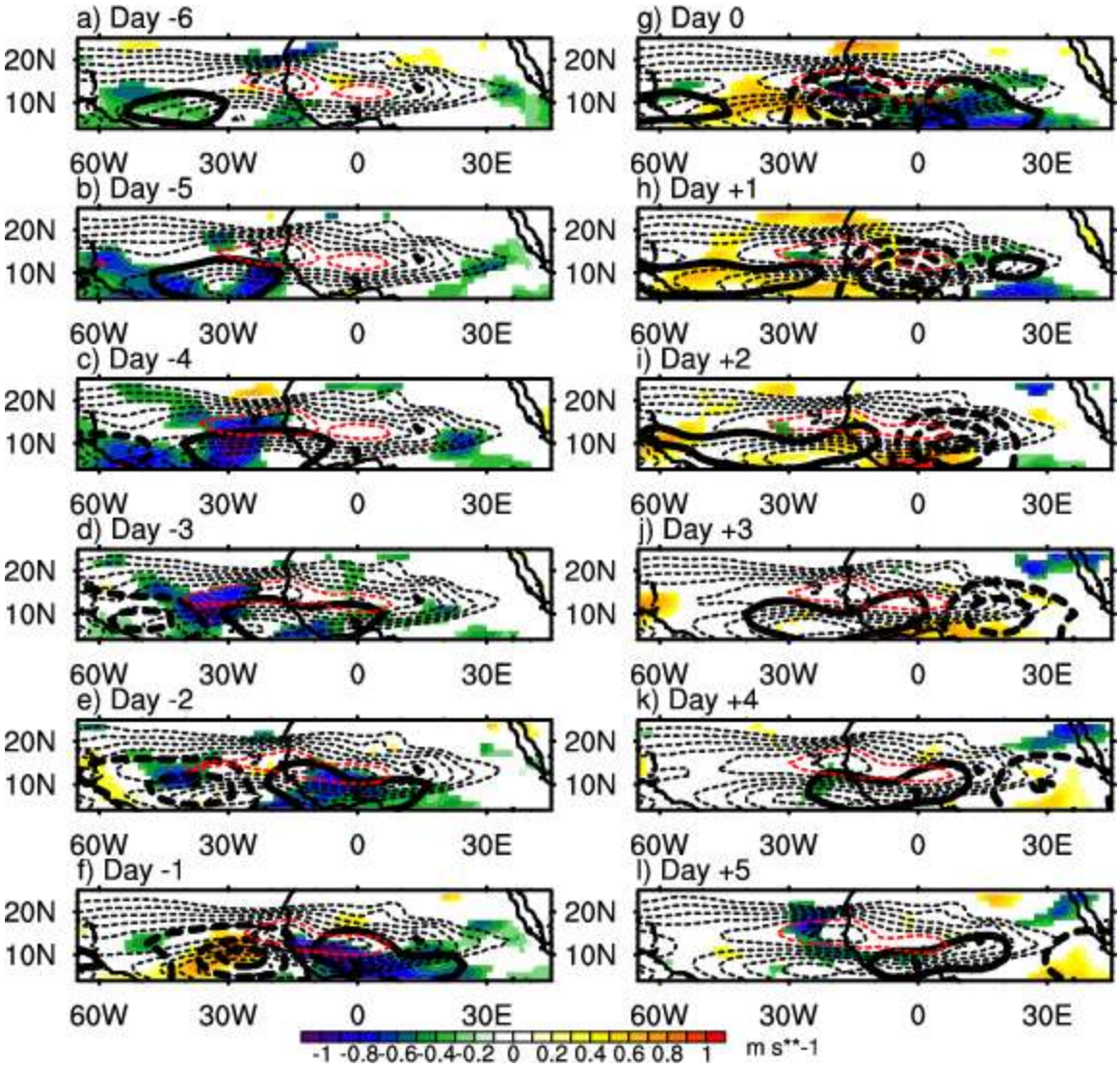

FIG. 5. 700 hPa zonal wind anomalies averaged over each CCKW lag. Anomalies statistically significantly different than zero at the 95% level are shaded. Total raw easterly zonal wind is composited for each CCKW lag and contoured. Kelvin filtered OLR anomalies are contoured (bold). Negative Kelvin filtered OLR anomalies are dashed. Shade interval is 0.2 ms^{-1}; Kelvin filtered OLR contour interval is 3 Wm^{-2}; easterly 700 hPa winds contour range is from -10 to -4 ms^{-1}; wind contour interval is 1 ms^{-1}. The red dashed contour highlights the -9 ms^{-1} contour.

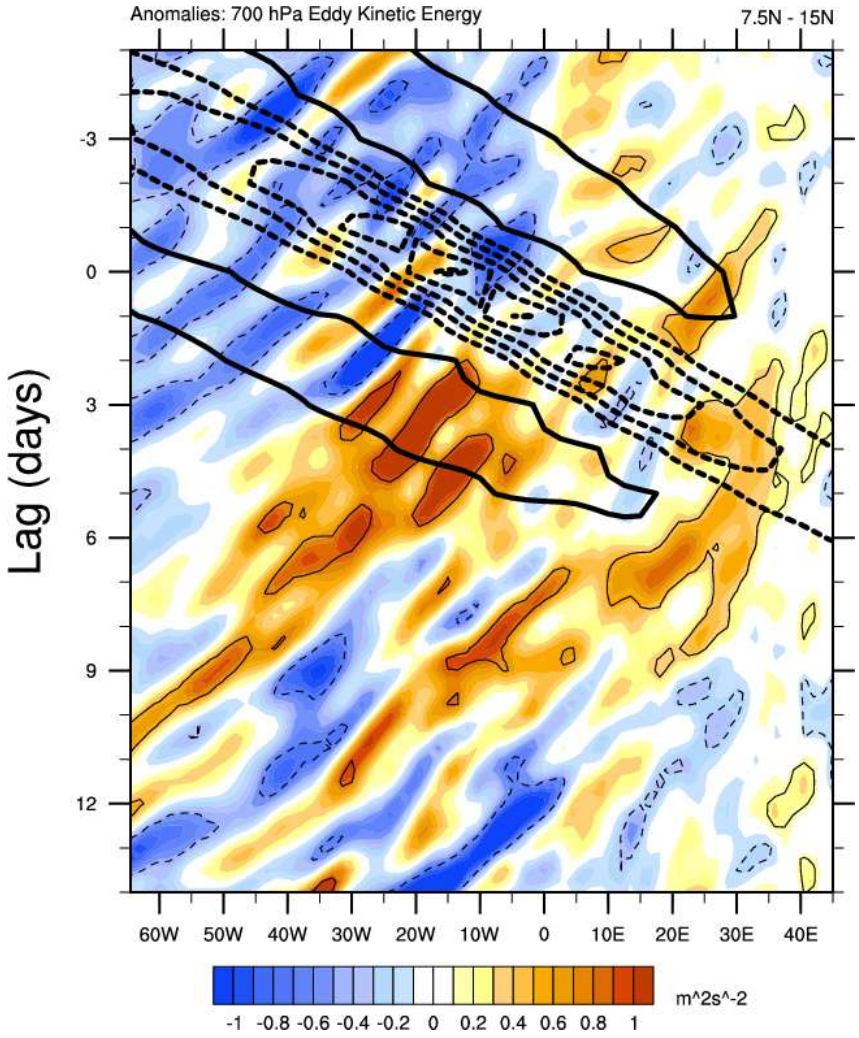

FIG. 6. A time-longitude composite of 2-10 day filtered 700 hPa eddy kinetic energy (shaded) averaged and over each lag of the CCKW index between the 7.5-15˚N band. Positive (Negative) eddy kinetic energy anomalies statistically different than zero at the 90% level are within the solid (dashed) contour. Kelvin filtered OLR anomalies are averaged over the 5-10˚N latitude band and are boldly contoured. Negative Kelvin filtered OLR anomalies are dashed. Shade interval is 0.1 m^2s^{-2}; contour interval is 3 Wm^{-2}.

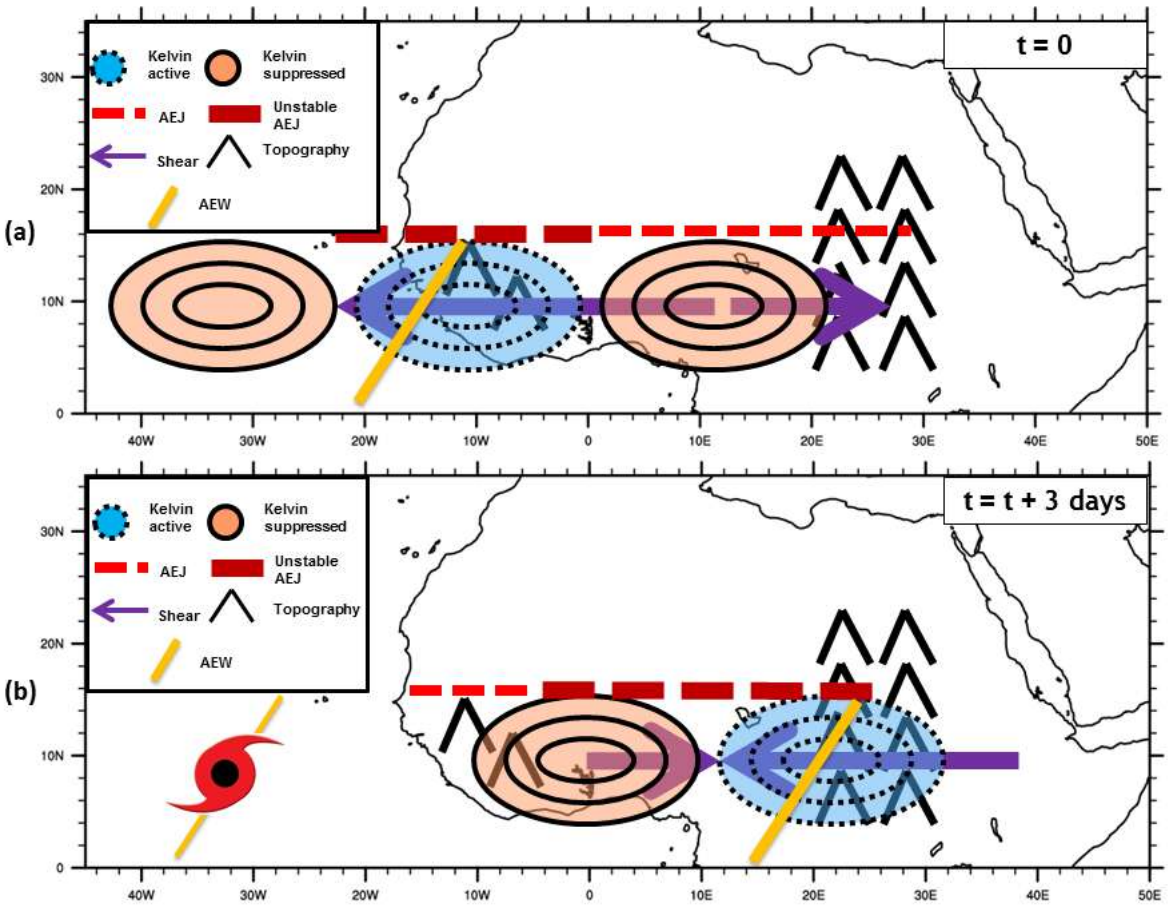

FIG. 7. A schematic diagram representing the modulation of the African environment and AEW activity by the passage of a CCKW when the convective envelope of the CCKW is over (a) the Guinea Highlands and (b) approximately three days later when it is over the eastern African highlands.